Journal of Nepal Mathematical Society (JNMS)
ISSN: 2616-0153 (Print), 2616-0161 (Online)
Vol. 9, Issue 1, 2026 (June): 48-59
DOI: https://doi.org/10.3126/jnms.v9i1.95969

Research Article
Received Date: April 8, 2026
Accepted Date: June 12, 2026
Published Date: June 25, 2026

Co-Axial Cylindrical Model for Turbulent Airflow and Laminar Mucus Flow in Constricted Lung Airways

Kritika Singh[1],Vijai Shanker Verma[2], Vikash Rana[2], Janta Raut[3]

[1]Bharat Ratna Sardar Vallabh Bhai Patel Rajkiya Engineering College, Basti, India
[2]Deen Dayal Upadhyaya Gorakhpur University, Gorakhpur, India
[3]Thakur Ram Multiple Campus, Tribhuvan University, Birgunj, Nepal

Correspondence to: Janta Raut, Email: janta.raut@trmc.tu.edu.np

Abstract: *This paper presents a two-layer cylindrical quasi-steady co-axial flow model of air and mucus in constricted airways that is affected by a time-varying pressure gradient. In this model both air and mucus are treated as incompressible Newtonian fluids. The air is considered to flow under quasi-steady state turbulent conditions whereas the mucus is assumed to flow under quasi steady-state laminar conditions. The model includes the effect of the immotile cilia layer by considering a slip condition at the airway wall. This makes the model more realistic and helps to better describe the interaction between airflow and mucus in narrowed airways than conventional no-slip models. The analysis indicates that both air and mucus flow rates decrease as the viscosity of mucus and constriction thickness increases. The analysis also indicates that both air and mucus flow rates increase with a higher pressure gradient and slip parameter. These findings provide insight into mucus clearance mechanisms in obstructive respiratory diseases such as asthma, chronic bronchitis, COPD and tracheal stenosis.*

Keywords: Quasi-steady state, Turbulent flow, Time varying pressure gradient, Immotile cilia, Constricted airways

1 Introduction

The human respiratory system comprises the upper respiratory tract and the lower respiratory tract. The upper respiratory tract consists of the nose, nasal cavity, pharynx and related structures, while the lower respiratory tract includes the larynx, trachea, bronchi, bronchioles and associated structures. The lungs contain the lower part of the respiratory tract known as the bronchial tree, a complex network of branching tubes that start at the trachea and further divide into two bronchi and continue to the alveoli, where gas exchange occurs with the cardiovascular system. In regular respiration, the airways deliver inspired air to the lungs while also allowing entry of dust, toxic gases, and microbial particles. Many of these particles settle in the lower airways. They are retained in the mucus lining and eventually eliminated from the system. Mucus production and the continuous transport of mucus from the lower airways to the oropharynx serve as effective defense mechanisms that help clear the airways of foreign materials and maintain the sterility of the lungs through coughing. Coughing is a physiological response observed in both healthy individuals and those with certain medical conditions. Diseases such as cystic fibrosis, chronic bronchitis, bronchial asthma, lung cancer, ciliary dyskinesia and tracheal stenosis can negatively affect the human lungs when they are exposed to these conditions. In many of these diseases, the cilia become immotile and thus resulting in their loss.

Human respiratory tracts are extremely sensitive, breathing in dust, straw, or carcinogens like irritants may cause sneezing and inflammation in the airways. This causes trigger forced expiration or coughing so that mucus and air can flow through the airways. Coughing plays a protective role by preventing aspiration into the lungs and aiding the transport of secretions and other substances upward through the respiratory tract [16].

Over the last several decades, many studies have investigated two-phase flow in respiratory tubes under externally applied pressure to stimulate the transport of mucus in the airways during coughing. Clarke et al. [4] found that liquid-lined tubes exhibited a significant increase in airflow resistance at all flow rates compared to dry tubes. They also noted that the non-linear pressure-flow relationships in liquid lined tubes under laminar flow conditions were due to the higher flow resistance caused by the presence of high-viscosity

fluid in the air passages.

Verma and Rana [23] presented a steady-state mathematical model of mucus transport in human lung airways, considering airflow, ciliary activity, and porosity, with mucus assumed to behave as a viscoelastic fluid. They demonstrated that the mucus transport rate increases with higher air flow, cilia activity and porosity, while decreasing with higher viscosities of the serous and mucus layers. Kumar et al. [7] explored mucus transport in diseased airways by examining the impact of constriction on the airways showing that the mucus transport rate decreases as the airway constriction increases. Chitra and Shabana [3] offered a two-layer model for the air-mucus interface in constricted human airways under a time-varying pressure gradient by considering the effect of slip parameter. They observed that the mucus flow rate increases with an increase in the slip parameter. Rana et al. [11] proposed a two-layer circular steady-state mathematical model to examine mucus flow in the lung airways,incorporating viscoelastic mucus behavior, ciliary activity, and porous medium effects. Padmavathi and Selvi [10] introduced two dimensional unsteady incompressible viscous laminar Newtonian fluid surrounded by the layers of porous tissue. They simulated mathematical model to express the pulmonary edema infection. They found that mucus flow rate increases as elastic parameter and resistance parameter decrease. Raut [12] presented a two-layer circular unsteady state mathematical model for mucus transport in the human lung airways resulting from coughing. The model incorporates the roles of air flow velocity and porosity parameter on mucus transport under the influence of time varying pressure gradient due to coughing. The model shows that the mucus transport rate decreases with increasing mucus viscosity and elastic modulus, while it increases with higher airflow velocity, porosity, mucus layer thickness, and pressure gradient. Modaresi and Shirani [8] presented a two-dimensional unsteady an incompressible mathematical model to evaluate mucus layer velocity in respiratory tracts. This model includes free-slip condition, cough shear stress, sneeze shear stress and shear stress of laminar airflow. They obtained that mucociliary transport is reduced as the thickness of the mucus layer grows. Raut et al. [13] formulated a mathematical model to study mucus flow rate in the human lung airways. The model incorporates the effects of cilia beating, porosity and shear stress generated by air-motion due to force expiration. The results show that mucus transport rate is positively correlated with pressure drop, shear stress, and porosity, and negatively correlated with mucus density and elastic modulus.

Most existing studies have focused on steady or laminar airflow and have not considered the combined effects of turbulent airflow, airway constriction and slip effects. Since airflow may become turbulent during coughing a more comprehensive model is required to accurately describe mucus transport in constricted airways. Therefore, the objective of this study is to develop and analyze a two-layer cylindrical co-axial flow model incorporating turbulent airflow, airway constriction and slip effects to investigate their influence on airflow and mucus transport during mild coughing.

In this study, we assume that the airflow in the central core lumen is of quasi-steady and turbulent type whereas mucus flow surrounding the core lumen is assumed as quasi-steady state and laminar. We took into account the impact of the slip parameter caused by the immotile cilia, which form a porous matrix in contact with epithelial walls. Here, we use air and mucus flow as co-axial and symmetrical around the central line of the airways. We consider the applied pressure gradient as a time-varying function representing mild cough. We also consider mucus as an incompressible Newtonian fluid [26] and airflow as turbulent during coughing [17]. We assume mucus directly attached to the epithelial walls. We also assume immotile cilia bed saturated with watery serous fluid governed by Darcy's law.

2 Methodology

In this paper, airflow is assumed to be turbulent because airflow velocity during coughing can become sufficiently high in the larger airways to induce turbulence. The mucus layer is modelled as a Newtonian fluid since several studies have shown that under moderate shear conditions mucus can be approximated as Newtonian. The airway geometry is assumed to be cylindrical and axisymmetric to simplify the mathematical formulation while retaining the essential characteristics of airflow–mucus interaction. The immotile cilia layer is represented as a porous medium governed by Darcy's law which provides a simplified description of fluid motion through the ciliary bed.

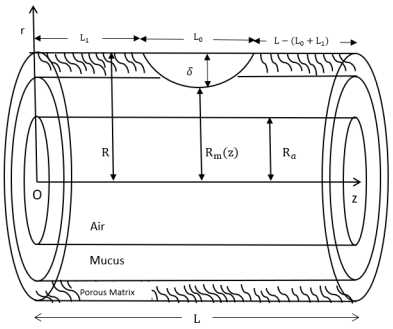

Figure 1: Cylindrical tube geometry for mucus transport in constricted lung airways

Mathematical Model

In reality, the airways of the human lungs exhibit a cylindrical geometry. Therefore, the flow of air and mucus in a lung airway is represented by a co-axial cylindrical tube geometry with ciliated inner surface wall as shown in Figure 1. The airway lumen is assumed to contain a central region filled with air and enclosed by a thick mucus layer. Due to the instantaneous pressure gradient induced by coughing, the airflow in the core region is modeled as quasi-steady turbulent flow, whereas the surrounding mucus layer is assumed to undergo quasi-steady laminar flow. The model also takes into account the influence of a slip parameter induced by immotile cilia in the serous layer that form a porous matrix in contact with the epithelial wall. In pathological situations, the mucus layer may be constricted and tightened due to smooth muscles connected to the wall. The radius of the cylindrical tube varies with the constriction geometry and therefore, there exists following relation which gives the impact of constriction in the diseased state of the human lungs [20, 25]:

$$\frac{R_m(z)}{R} = \begin{cases} 1 - \frac{\delta}{2R}\{1 + cos\frac{2\pi}{L_0}\left(z - L_1 - \frac{L_0}{2}\right)\}, & L_1 \le z \le L_1 + L_0 \\ 1, & 0 \le z \le L_1 \quad \text{and} \quad L_1 + L_0 \le z \le L \end{cases} \tag{1}$$

where R is the radius of circular tube, $R_m(z)$ is the radius of circular tube in constricted area, $\delta(<< R_m(z))$ is the thickness of constriction which is sinusoidal.
Let $a = R - \frac{\delta}{2}$ and $b = \frac{\delta}{2}$, then equation (1) becomes:

$$R_m(z) = a - bcos\frac{2\pi}{L_0}\left(z - L_1 - \frac{L_0}{2}\right)$$

The assumption of turbulent airflow is based on literature review [18], which reported that airflow velocities during coughing can become sufficiently high in the larger airways to generate turbulent flow characteristics. Reynolds number exceeds 4000 and flow becomes turbulent. Under these conditions, turbulent shear stresses dominate over viscous stresses and significantly influence momentum transfer from the airflow to the mucus layer. Therefore, Prandtl's mixing length theory is adopted to describe the turbulent airflow region.

The governing equations for the air and mucus flows under the above said state in a cylindrical tube can be written as follows:
Region I: Air Flow Region $(0 \le r \le R_a)$

$$\frac{\partial p}{\partial z} = \frac{1}{r}\frac{\partial}{\partial r}(r\tau_a) \tag{2}$$

$$\tau_a = -\rho_a l_a^2 \left(-\frac{\partial u_a}{\partial r}\right)^2 \tag{3}$$

Region II: Mucus Flow Region $(R_a \leq r \leq R_m(z))$

$$\frac{\partial p}{\partial z} = \frac{1}{r}\frac{\partial}{\partial r}(r\tau_m) \tag{4}$$

$$\tau_m = \mu_m \frac{\partial u_m}{\partial r} \tag{5}$$

where z is the axial coordinate along the tube axis which is in the flow direction and r is the radial coordinate in the radial direction which is perpendicular to the fluid flow, R_a is the thickness upto air-mucus interface, p is the mean pressure that is constant across the two layers, τ_a and τ_m are the mean shear stress across air and mucus region, ρ_a is the density of air, u_a and u_m are the mean velocity components of the air and mucus in the direction of z and μ_a, μ_m are the viscosities of air and mucus respectively.

By using Prandtl mixing length theory, l_a is assumed as

$$l_a = l_0(R - r) \tag{6}$$

where l_0 is constant and determined experimentally [18].
The following boundary and matching conditions are taken into account to solve the problem:
Boundary Conditions:

$$\frac{\partial u_a}{\partial r} = 0, \quad r = 0 \tag{7}$$

$$u_m = -\beta\tau_m, \quad r = R_m(z) \tag{8}$$

Matching Conditions:

$$u_a = u_m, \quad r = R_a \tag{9}$$

$$\tau_a = \tau_m, \quad r = R_a \tag{10}$$

The negative sign in equation (8) is considered due to the negative value of τ_m in the mucus layer. This condition involves the sudden constriction of the muscles surrounding the airways, leading to a rapid change in the velocity gradient. The negative sign in the shear stress equation indicates the direction of the stress opposing the airflow, which is essential for understanding the mechanical forces during constriction. Here, it is important to emphasize that β is the slip parameter at the boundary between mucus and immotile cilia. Since the cilia are immersed in a serous fluid layer and form a porous matrix, a limited relative motion may occur between the mucus and the airway wall. Consequently, a slip condition is considered more appropriate than the conventional no-slip condition for describing mucus transport near the wall [19].

During coughing, the pressure gradient generated in lung airways changes with time. Therefore, we may assume that

$$-\frac{\partial p}{\partial z} = P = P_0 f(t), \tag{11}$$

where t represents time and P_0 is constant affected by the intensity of the mild cough. The magnitude of the mild cough is dependent upon the intensity of the turbulence caused by the cough. A cough that is more intense causes a corresponding increase in flow rates. If there is not even a slight cough, P is zero everywhere. However, mucus transport continues to occur because of the mean velocity of the cilia beating [15]. The function $f(t)$ characterizes the mild cough [7] and is defined as:

$$f(t) = \begin{cases} \frac{3t^2}{8T_m}\left(1 - \frac{2t}{3T_m}\right), & 0 \leq t \leq T_m \\ \frac{9t}{32}\left(1 - \frac{9t}{10T}\right)^2, & T_m \leq t \leq \frac{T}{\alpha} \\ 0, & \frac{T}{\alpha} \leq t \end{cases} \tag{12}$$

where $\alpha = 0.9$ and $T_m = 0.011$ is the time when $f(t)$ is maximum. To simplify the analysis, we can assume the cough duration T spans from 0.030 seconds to 0.032 seconds. The graphical representation of equation (12) is shown in Figure 2.

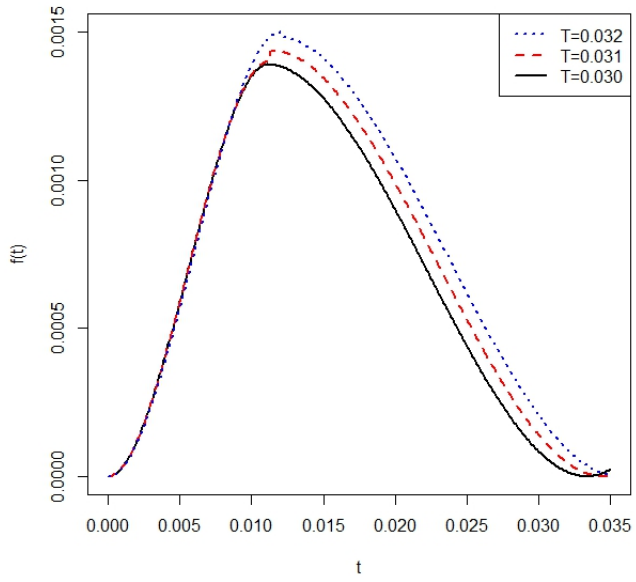

Figure 2: Graphical Representation of $f(t)$ for different values of T

3 Analytical Solution

Solving equations (2)-(5) by using boundary and matching conditions (7)-(10), the stress and velocity components in air and mucus layers are computed which are given below:

$$\tau_a = \tau_m = -\frac{Pr}{2} \tag{13}$$

$$u_a = \frac{P}{4\mu_m}[R_m^2(z) + 2\beta\mu_m R_m(z) - R_a^2] + \sqrt{\frac{PR}{2\rho_a l_0^2}}\left[\log\left|\frac{\sqrt{R}+\sqrt{R_a}}{\sqrt{R}-\sqrt{R_a}}\right| - \log\left|\frac{\sqrt{R}+\sqrt{r}}{\sqrt{R}-\sqrt{r}}\right| + \frac{2(\sqrt{r}-\sqrt{R_a})}{\sqrt{R}}\right] \tag{14}$$

$$u_m = \frac{P}{4\mu_m}[R_m^2(z) + 2\beta\mu_m R_m(z) - r^2] \tag{15}$$

The volumetric flow rates in the two layers (air and mucus) can be defined as follows:

$$Q_a = \int_0^{R_a} 2\pi r u_a dr \tag{16}$$

$$Q_m = \int_{R_a}^{R_m(z)} 2\pi r u_m dr \tag{17}$$

Substituting the values of u_a from (14) and u_m from (15) in equation (16) and (17) respectively, we get

$$\frac{Q_a}{2\pi} = \frac{PR_a^2}{8\mu_m}\left(R_m^2(z) + 2\beta\mu_m R_m(z) - R_a^2\right) + \sqrt{\frac{PR^5}{8\rho_a l_0^2}}\left[\log\left|\frac{\sqrt{R}+\sqrt{R_a}}{\sqrt{R}-\sqrt{R_a}}\right| - 2\sqrt{\frac{R_a}{R}}\left(1 + \frac{R_a}{3R} + \frac{R_a^2}{5R^2}\right)\right] \tag{18}$$

$$\frac{Q_m}{2\pi} = \frac{P}{16\mu_m}\left(R_m^2(z) - R_a^2\right)\left(R_m^2(z) + 4\beta\mu_m R_m(z) - R_a^2\right) \tag{19}$$

To calculate the pressure drop in each layer, we understand from the equation of continuity that both Q_a and Q_m are constants. Therefore, from (18) and (19), we get

$$-\frac{\partial p}{\partial z} = \frac{64\mu_m^2 K_2^2}{R_a^4\left(R_m^2(z)+K_1R_m(z)-R_a^2\right)^2} + \frac{Q_a}{\pi}\left[\frac{8\mu_m}{R_a^2\left(R_m^2(z)+K_1R_m(z)-R_a^2\right)}\right] \tag{20}$$

$$-\frac{\partial p}{\partial z} = \frac{Q_m}{\pi K_3\left(R_m^2(z)-R_a^2\right)\left(R_m^2(z)+2K_1R_m(z)-R_a^2\right)} \tag{21}$$

where,

$$K_1 = 2\beta\mu_m, K_2 = \sqrt{\frac{R^5}{8\rho_a l_0^2}}\left[\log\left|\frac{\sqrt{R}+\sqrt{R_a}}{\sqrt{R}-\sqrt{R_a}}\right| - 2\sqrt{\frac{R_a}{R}}\left(1+\frac{R_a}{3R}+\frac{R_a^2}{5R^2}\right)\right],$$

$$K_3 = \frac{1}{8\mu_m}.$$

Replacing $R_m(z)$ by R for non-constricted regions ($0 \le z \le L_1$ and $L_1 + L_0 \le z \le L$). Then the pressure gradient for non-constricted regions becomes

$$-\frac{\partial p}{\partial z} = \frac{64\mu_m^2 K_2^2}{R_a^4\left(R^2+K_1R-R_a^2\right)^2} + \frac{Q_a}{\pi}\left[\frac{8\mu_m}{R_a^2\left(R^2+K_1R-R_a^2\right)}\right] \tag{22}$$

$$-\frac{\partial p}{\partial z} = \frac{Q_m}{\pi K_3\left(R^2-R_a^2\right)\left(R^2+2K_1R-R_a^2\right)} \tag{23}$$

Since the pressure is present only at two ends of the tube i.e.,$p = p_0$ at $z = 0$, $p = p_L$ at $z = L$. Then, we define the pressure drop as $\Delta P = p_0 - p_L$.
Now, integrating equations (20) and (22), we get

$$\begin{aligned}\Delta P = -\int_0^L dp = &\int_0^{L_1}\left[\frac{64\mu_m^2K_2^2}{R_a^4\left(R^2+K_1R-R_a^2\right)^2} + \frac{Q_a}{\pi}\frac{8\mu_m}{R_a^2\left(R^2+K_1R-R_a^2\right)}\right]dz\\ &+\int_{L_1}^{L_1+L_0}\left[\frac{64\mu_m^2K_2^2}{R_a^4\left(R_m^2(z)+K_1R_m(z)-R_a^2\right)^2} + \frac{Q_a}{\pi}\frac{8\mu_m}{R_a^2\left(R_m^2(z)+K_1R_m(z)-R_a^2\right)}\right]dz\\ &+\int_{L_1+L_0}^{L}\left[\frac{64\mu_m^2K_2^2}{R_a^4\left(R^2+K_1R-R_a^2\right)^2} + \frac{Q_a}{\pi}\frac{8\mu_m}{R_a^2\left(R^2+K_1R-R_a^2\right)}\right]dz\end{aligned}$$

Putting the value of $R_m(z)$ from (1) in above equation, we get

$$\begin{aligned}\Delta P = &\frac{64\mu_m^2K_2^2(L-L_0)}{R_a^4\left(R^2+K_1R-R_a^2\right)^2} + \frac{64\mu_m^2K_2^2L_0}{R_a^4(n-m)^2}\left[\frac{a+m}{((a+m)^2-b^2)^{3/2}} + \frac{a+n}{((a+n)^2-b^2)^{3/2}}\right]\\ &+\frac{128\mu_m^2K_2^2L_0}{R_a^4(n-m)^3}\left[\frac{1}{((a+n)^2-b^2)^{1/2}} - \frac{1}{((a+m)^2-b^2)^{1/2}}\right] + \frac{Q_a}{\pi}\frac{8\mu_m(L-L_0)}{R_a^2\left(R^2+K_1R-R_a^2\right)}\\ &+\frac{Q_a}{\pi}\frac{8\mu_mL_0}{R_a^2(n-m)}\left[\frac{1}{((a+m)^2-b^2)^{1/2}} - \frac{1}{((a+n)^2-b^2)^{1/2}}\right]\end{aligned} \tag{24}$$

where $m = \frac{K_1}{2} + \sqrt{R_a^2 + \frac{K_1^2}{4}}$ and $n = \frac{K_1}{2} - \sqrt{R_a^2 + \frac{K_1^2}{4}}$
Let

$$X_1 = \frac{8\mu_m(L-L_0)}{R_a^2\left(R^2+K_1R-R_a^2\right)} + \frac{Q_a}{\pi}\frac{8\mu_mL_0}{R_a^2(n-m)}\left[\frac{1}{((a+m)^2-b^2)^{1/2}} - \frac{1}{((a+n)^2-b^2)^{1/2}}\right]$$

$$\begin{aligned}Y_1 = &\frac{64\mu_m^2K_2^2(L-L_0)}{R_a^4\left(R^2+K_1R-R_a^2\right)^2} + \frac{64\mu_m^2K_2^2L_0}{R_a^4(n-m)^2}\left[\frac{a+m}{((a+m)^2-b^2)^{3/2}} + \frac{a+n}{((a+n)^2-b^2)^{3/2}}\right]\\ &+\frac{128\mu_m^2K_2^2L_0}{R_a^4(n-m)^3}\left[\frac{1}{((a+n)^2-b^2)^{1/2}} - \frac{1}{((a+m)^2-b^2)^{1/2}}\right]\end{aligned}$$

then the equation (24) becomes

$$\Delta P = Y_1 + \frac{Q_a}{\pi} X_1 \tag{25}$$

The volumetric flow rate in air region i.e. Q_a can be found as follows

$$Q_a = \pi \frac{(\Delta P - Y_1)}{X_1} \tag{26}$$

Similarly, integrating equation (21) and (23), we get

$$\begin{aligned}\Delta P = -\int_0^L dp = \int_0^{L_1} & \frac{Q_m dz}{\pi K_3 \left(R^2 - R_a^2\right)\left(R^2 + 2K_1 R - R_a^2\right)} \\ & + \int_{L_1}^{L_1+L_0} \frac{Q_m dz}{\pi K_3 \left(R_m^2(z) - R_a^2\right)\left(R_m^2(z) + 2K_1 R_m(z) - R_a^2\right)} \\ & + \int_{L_1+L_0}^{L} \frac{Q_m dz}{\pi K_3 \left(R^2 - R_a^2\right)\left(R^2 + 2K_1 R - R_a^2\right)}\end{aligned}$$

After putting the value of $R_m(z)$ from (1) in above equation, we get

$$\begin{aligned}\Delta P = & \frac{Q_m}{\pi K_3}\left\{\frac{(L-L_0)}{(R^2-R_a^2)^2 + 2K_1R(R^2-R_a^2)} + \frac{L_0}{4R_a^2K_1}\left[\frac{1}{((a+R_a)^2-b^2)^{1/2}} + \frac{1}{((a-R_a)^2-b^2)^{1/2}}\right]\right\} \\ & + \frac{Q_m}{\pi K_3}\left\{\frac{L_0}{4K_1(R_a^2+K_1^2)^{1/2}}\left[\frac{1}{v((a+v)^2-b^2)^{1/2}} - \frac{1}{u((a+u)^2-b^2)^{1/2}}\right]\right\}\end{aligned} \tag{27}$$

where $u = K_1 + \sqrt{K_1^2 + R_a^2}$ and $v = K_1 - \sqrt{K_1^2 + R_a^2}$.
Let

$$X_2 = \frac{(L-L_0)}{(R^2-R_a^2)^2 + 2K_1R(R^2-R_a^2)} + \frac{L_0}{4R_a^2K_1}\left[\frac{1}{((a+R_a)^2-b^2)^{1/2}} + \frac{1}{((a-R_a)^2-b^2)^{1/2}}\right]$$

$$Y_2 = \frac{L_0}{4K_1(R_a^2+K_1^2)^{1/2}}\left[\frac{1}{v((a+v)^2-b^2)^{1/2}} - \frac{1}{u((a+u)^2-b^2)^{1/2}}\right]$$

then the equation (27) becomes

$$\Delta P = \frac{Q_m}{\pi K_3}(X_2 + Y_2)$$

The volumetric flow rate in mucus region i.e. Q_m can be found as follows:

$$Q_m = \frac{\pi K_3 \Delta P}{(X_2 + Y_2)} \tag{28}$$

4 Results and Discussion

To explore the impact of various model parameters on flow rates of air and mucus in trachea, the values of Q_a and Q_m as provided by equations (26) and (28) were calculated using the following dataset [21, 24]:

$R = 90.00 \times 10^{-2}$ cm
$R_m = 38.45 \times 10^{-2}$ cm
$R_a = 31.45 \times 10^{-2}$ cm
$t = 0 - 0.035$ sec
$T = 0.030$ sec
$L = 1.0$ cm
$L_0 = 0.5$ cm
$l_0 = 0.40$
$P_0 = (1 - 10) \times 10^5$ gm cm^{-2} sec^{-2}
$\mu_m = 1.00 - 10.00$ poise
$\mu_a = 0.0002$ poise
$\rho_a = 1.00 \times 10^{-3}$gm cm^{-3}
$\beta = 0 - 0.10$ gm cm^2 sec
$\delta = 0 - 0.1$ cm

The variations in volumetric flow rates Q_a and Q_m with respect to time t are shown in following figures:

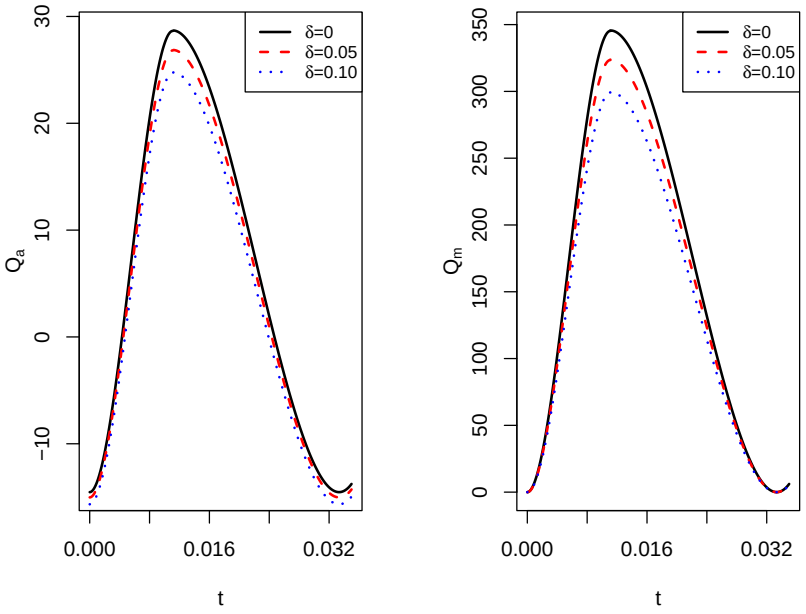

Figure 3: Variations in Q_a and Q_m with t for distinct values of δ

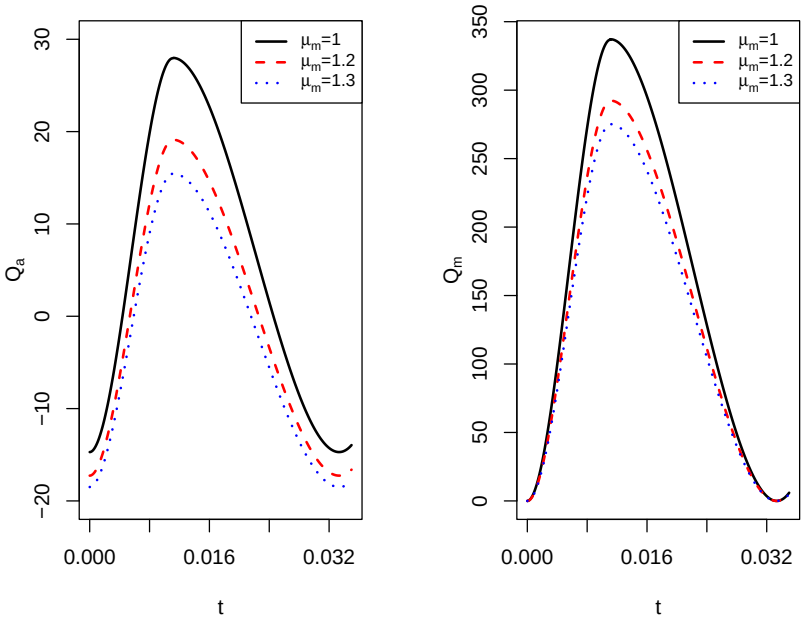

Figure 4: Variations in Q_a and Q_m with t for distinct values of μ_m

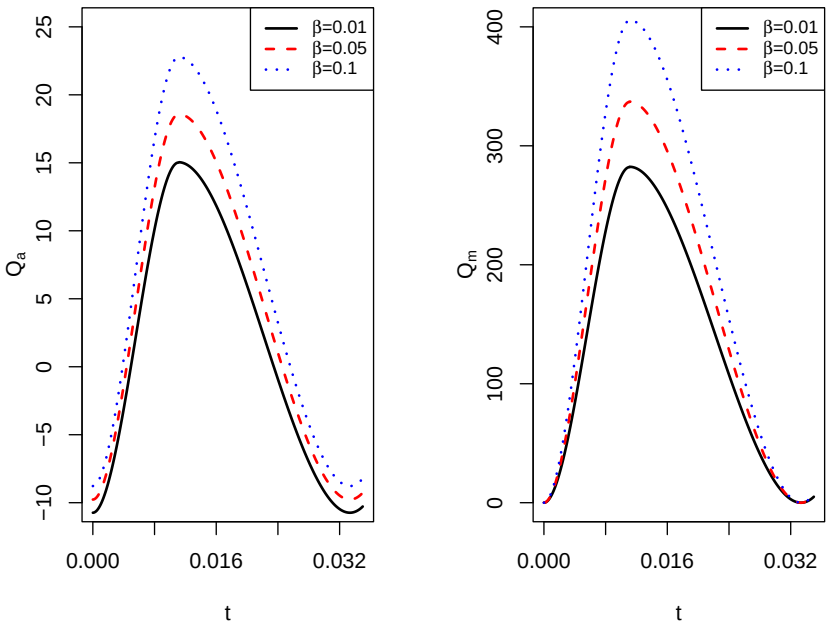

Figure 5: Variations in Q_a and Q_m with t for distinct values of β

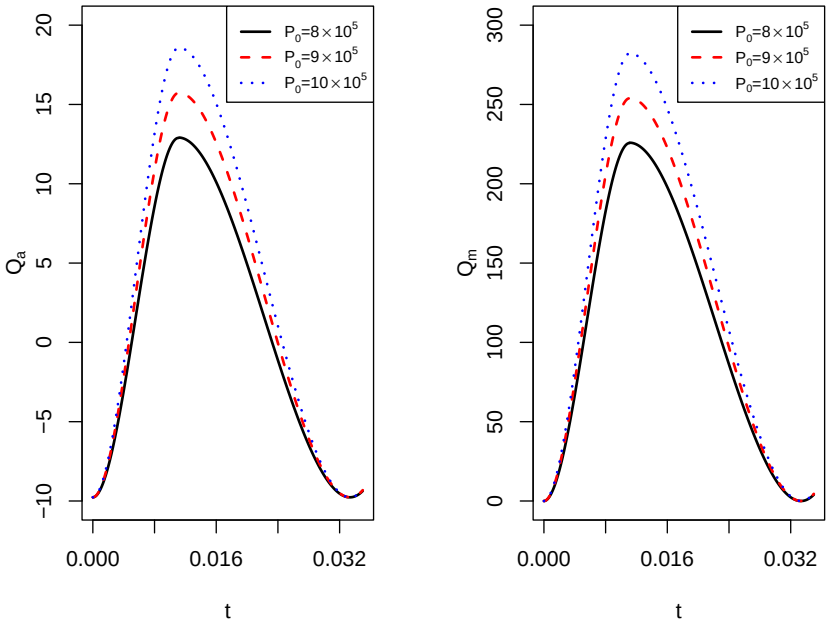

Figure 6: Variations in Q_a and Q_m with t for distinct values of P_o

Figure 3 illustrates the impact of time on the flow rates of air and mucus for fixed values of $T = 0.035$ sec, $L = 1$ cm, $L_0 = 0.5$ cm, $R = 90.00 \times 10^{-2}$ cm, $R_m = 38.45 \times 10^{-2}$ cm, $R_a = 31.45 \times 10^{-2}$ cm, $\mu_m = 1$ poise, $\rho_a = 1.00 \times 10^{-3}$ gm cm^{-3}, $\beta = 0.05$ gm cm^{2}sec, $P_0 = 10 \times 10^5$ gm cm^{-2} sec^{-2}and $\mu_a = 0.0002$ poise for different values of δ. It is noted that as constriction thickness increases, the volumetric flow rates of mucus and air decrease. These results are consistent with previous findings [7, 19]. This suggests that airway narrowing significantly impairs mucus clearance and airflow which may contribute to airway obstruction and respiratory complications in diseases such as asthma, COPD and tracheal stenosis.

Figure 4 shows the impact of time on air and mucus flow rates for fixed values of $T = 0.035$ sec, $L = 1$ cm, $L_0 = 0.5$ cm, $R = 90.00 \times 10^{-2}$ cm, $R_m = 38.45 \times 10^{-2}$ cm, $R_a = 31.45 \times 10^{-2}$ cm, $\beta = 0.05$ gm cm^{2}sec, $P_0 = 10 \times 10^5$ gm cm^{-2} sec^{-2}, $\delta = 0.01$ cm, $\rho_a = 1.00 \times 10^{-3}$ gm cm^{-3} and $\mu_a = 0.0002$ poise for various values of μ_m. The observation reveals that air and mucus flow rates decrease with increase in mucus viscosity. These results are consistent with previous findings [22, 23]. These findings indicate that highly viscous mucus can impair mucociliary clearance, promote mucus accumulation and worsen pulmonary function in chronic bronchitis, asthma and other mucus-related respiratory disorders.

Figure 5 depicts the impact of time on air and mucus flow rates for fixed values of $T = 0.035$ sec, $L = 1$ cm, $L_0 = 0.5$ cm, $R = 90.00 \times 10^{-2}$ cm, $R_m = 38.45 \times 10^{-2}$ cm, $R_a = 31.45 \times 10^{-2}$ cm, $\mu_m = 1$ poise, $P_0 = 10 \times 10^5$ gm cm^{-2} sec^{-2}, $\delta = 0.01$ cm, $\rho_a = 1.00 \times 10^{-3}$ gm cm^{-3} and $\mu_a = 0.0002$ poise for different values of β. It is observed that air and mucus flow rates increase as the slip parameter β increases. These results are consistent with previous findings [9, 14, 15]. Enhanced slip reduces wall resistance and facilitates mucus movement, thereby improving airway clearance and reducing the likelihood of mucus blockage in diseased airways.

Figure 6 depicts the impact of time on air and mucus flow rates for fixed values of $T = 0.030$ sec, $L = 1$ cm, $L_0 = 0.5$ cm, $R = 90.00 \times 10^{-2}$ cm, $R_m = 38.45 \times 10^{-2}$ cm, $R_a = 31.45 \times 10^{-2}$ cm, $\mu_m = 1$ poise, $\beta = 0.05$ gm cm^{2}sec, $\delta = 0.01$ cm, $\rho_a = 1.00 \times 10^{-3}$ gm cm^{-3}, $\mu_a = 0.0002$ poise and $\mu_m = 1$ poise for different values of P_0. It is observed that air and mucus flow rates increase as the pressure drop in the two layers increases. These results are consistent with previous findings [1, 2, 14]. This finding highlights the important role of coughing-induced pressure gradients in enhancing mucus clearance and maintaining airway patency under constricted airway conditions.

5 Model Validation

The validity of this model is assessed by comparing the predicted trends with previously published theoretical and experimental studies. The model predicts that airflow and mucus transport decrease with increasing constriction thickness and mucus viscosity, whereas both quantities increase with increasing slip parameter and pressure gradient. These observations are consistent with the findings reported in [1, 3, 18, 19], thereby providing qualitative validation of the proposed model. A sensitivity analysis was performed by varying the key model parameters individually while keeping the remaining parameters fixed. The results indicate that airflow and mucus transport are highly sensitive to changes in constriction thickness and mucus viscosity. An increase in either parameter leads to a significant reduction in transport due to increased flow resistance. In contrast, increasing the slip parameter and pressure gradient enhances both airflow and mucus transport by reducing wall resistance and increasing the driving force for flow. These observations suggest that airway narrowing and mucus rheology play dominant roles in determining mucus clearance efficiency in constricted airways.

6 Limitations

Although the model captures the essential features of airflow–mucus interaction, it is based on an idealized cylindrical geometry and assumes Newtonian mucus behaviour. Furthermore, airway branching, wall motion and three-dimensional flow effects are neglected. Future studies may incorporate non-Newtonian mucus properties, patient-specific airway geometries obtained from medical imaging, and computational fluid dynamics simulations to provide a more realistic representation of respiratory airflow and mucus transport.

7 Conclusion

This study presents a two-layer cylindrical co-axial flow model incorporating turbulent airflow and slip effects to investigate airflow and mucus transport in constricted lung airways during mild coughing. The results show that increasing constriction thickness and mucus viscosity reduce airflow and mucus transport, whereas increasing the slip parameter and pressure gradient enhance transport. These findings provide insight into mucus clearance and airway obstruction in respiratory diseases such as asthma, chronic bronchitis, COPD and tracheal stenosis.

Acknowledgement

The authors are thankful to Referees for valuable comments and suggestions.

References

[1] Agarwal, M., King, M., Rubin, B. K., and Shukla, J. B., 1989, Mucus transport in a miniaturized simulated cough machine: effect of constriction and serous layer stimulant, *Biorheology*, 26, 977-988.

[2] Agarwal, M., King, M., and Shukla, J. B., 1994, Mucus gel transport in a simulated cough machine: effects of longitudinal grooves representing spacings between arrays of cilia, *Biorheology*, 31, 11-19.

[3] Chitra, M., and Shabana, S., 2017, Two layered model of air mucus interface through constricted human airways under the influence of time varying pressure gradient, *International Conference on Mathematical Impacts in Science and Technology*, 17, 93-98.

[4] Clarke, S. W., Jones, J. G., and Oliver, D. R., 1970, Resistance to two-phase gas-liquid flows in airways, *J. Appl. Physiology*, 29(4), 464-471.

[5] Clarke, S. W., 1973, The role of two-phase flow in bronchial clearance, *Bull. Physiopath. Respir.*, 9(2), 359-376.

[6] King, M., Agarwal, M., and Shukla, J. B., 1993, A planar model for mucociliary transport: effect of mucus viscoelasticity, *Biorheology*, 30, 49-61.

[7] Kumar, P., Saxena, A., and Tyagi, A. P., 2016, Mathematical modelling of mucus transport in diseased airways with effects of constriction of airway diameter and mucus viscosity, *2016 3rd International Conference on Computing for Sustainable Global Development*, 1832-1836.

[8] Modaresi, M. A., and Shirani, E., 2023, Mucociliary clearance affected by mucus-periciliary interface stimulation using analytical solution during cough and sneeze, *The European Physical Journal Plus*, 138(201), 1-18.

[9] Nirmala P., and Chitra, M., 2014, Effects of air-mucus interface through a human trachea with mild constriction of aerosols, *International Journal of Innovative Research in Science Engineering and Technology*, 3-8.

[10] Padmavathi, T., and Selvi, S. S., 2021, The effect of mucociliary clearance on human lung mechanism in the presence of viscoelasticity, *International Journal of All Research Education and Scientific Methods*, 9(5), 3104-3111.

[11] Rana, V., Maurya, P. Bhadauria, A. S., and Verma, V. S., 2021, Effects of mucus visco-elasticity, cilia beating and porosity parameter on mucus transport in human lung airways, *Turkish Journal of Computer and Mathematics Education*, 12(12), 126-132.

[12] Raut, J., 2022, Roles of airflow velocity and porosity parameter on mucus transport in the human lung airways under the influence of time varying pressure gradient, *Journal of National Academy of Mathematics India*, 36, 49-62.

[13] Raut, J., Verma, V.S., and Rana, V., 2023, Mathematical modelling approach for transport of serous fluid and mucus in human lung airways, *Journal of Rajasthan Academy of Physical Sciences*, 22(3 & 4), 257-270.

[14] Satpathi, D. K., Rathish Kumar, B. V., and Chandra, P., 1973, Unsteady-state laminar flow of viscoelastic gel and air in a channel: application to mucus transport in a cough machine simulating trachea, *Mathematical and Computer Modelling*, 38, 1-2.

[15] Satpathi, D. K., Ratnam, K. V., and Ramu, A., 2016, Model for mucus transport in the airways due to air motion: effect of slipperiness, *International Journal of Biomathematics*, 9, 5.

[16] Saxena, A., and Tyagi, A. P., 2015, Mucus transport in the larger airway due to prolonged mild cough: effect of serous fluid and cilia beating, *Chemical and Process Engineering Research*, 31, 62-69.

[17] Scherer, P. W., 1981, Mucus transport by cough, *Chest*, 80, 830-833.

[18] Schlichting, H., 1960, *Boundary Layer Theory*, McGraw-Hill Book Company, Inc., New York.

[19] Singh, Y., Shekhar, K., and Tyagi, A. P. , 2021, Mathematical modelling of mucus transport in airways due to cough: quasi-steady state turbulent condition, *Series on Biomechanics*, 35(3), 69-84.

[20] Shukla, J. B., Parihar, R. S., and Gupta, S. P., 1979, Effects of peripheral layer viscosity on blood flow through the artery with mild stenosis, *Bulletin of Mathematical Biology*, 42, 797-805.

[21] Shukla, J. B., Chandra, P., Satpathi, D. K., and King, M., 1999, Some mathematical model for mucus transport in lung due to forced expiration or cough, *Proc. International Conference on Frontiers of Biomechanics, Bangalore, India.*

[22] Verma, V. S., and Tripathee, S.,M., 2013, A planar model for muco-ciliary transport in the human lung: effects of mucus visco-elasticity, cilia beating and porosity, *IJMRS's Int J. Mathematical Modelling and Physical Sciences*, 01(01), 19-25.

[23] Verma, V. S., and Rana. V., 2015, Mucus transport in the human lungs: a mathematical analysis, *Journal of Rajasthan Academy of Physical Sciences*, 14(2), 145-156.

[24] Weibel, E. R., 1963, *Morphometry of human lung*, New York, Academic Press Inc.

[25] Young, D. F., 1968, Effect of a time dependent stenosis on flow through a tube, *Journal of Engineering for Industry*, 90, 248-254.

[26] Zahm, J. M., King, M., Duvivier, C., Pierrot, D., Girod, S., and Puchelle, E., 1991, Role of simulated repetitive coughing in mucus clearance, *Eur. J. Respir. Dis.*, 4, 311-315.